Cell PRESS
Immunity
Article

IκB$_{NS}$ Protein Mediates Regulatory T Cell Development via Induction of the Foxp3 Transcription Factor

Marc Schuster,[1] Rainer Glauben,[2] Carlos Plaza-Sirvent,[1] Lisa Schreiber,[4] Michaela Annemann,[1] Stefan Floess,[4] Anja A. Kühl,[3] Linda K. Clayton,[5] Tim Sparwasser,[6] Klaus Schulze-Osthoff,[7] Klaus Pfeffer,[8] Jochen Huehn,[4] Britta Siegmund,[2] and Ingo Schmitz[1,*]

[1]Systems-oriented Immunology and Inflammation Research, Helmholtz Center for Infection Research, 38124 Braunschweig, Germany, and Institute for Molecular and Clinical Immunology, Otto-von-Guericke University, 39120 Magdeburg, Germany
[2]Medizinische Klinik I
[3]Institute of Pathology
Charité Universitätsmedizin Berlin, 12203 Berlin, Germany
[4]Department of Experimental Immunology, Helmholtz Center for Infection Research, 38124 Braunschweig, Germany
[5]Department of Cancer Biology, Dana-Farber Cancer Institute and Department of Medicine, Harvard Medical School, Boston, MA 02215, USA
[6]Institute for Infection Immunology, TWINCORE, 30625 Hannover, Germany
[7]Interfaculty Institute for Biochemistry, Eberhard-Karls University, 72076 Tübingen, Germany
[8]Institute for Medical Microbiology and Hospital Hygiene, Heinrich-Heine University, 40225 Düsseldorf, Germany
*Correspondence: ingo.schmitz@helmholtz-hzi.de
http://dx.doi.org/10.1016/j.immuni.2012.08.023

SUMMARY

Forkhead box P3 positive (Foxp3$^+$) regulatory T (Treg) cells suppress immune responses and regulate peripheral tolerance. Here we show that the atypical inhibitor of NFκB (IκB) IκB$_{NS}$ drives Foxp3 expression via association with the promoter and the conserved noncoding sequence 3 (CNS3) of the *Foxp3* locus. Consequently, IκB$_{NS}$ deficiency leads to a substantial reduction of Foxp3$^+$ Treg cells in vivo and impaired Foxp3 induction upon transforming growth factor-β (TGF-β) treatment in vitro. Moreover, fewer Foxp3$^+$ Treg cells developed from IκB$_{NS}$-deficient CD25$^-$CD4$^+$ T cells adoptively transferred into immunodeficient recipients. Importantly, IκB$_{NS}$ was required for the transition of immature GITR$^+$CD25$^+$ Foxp3$^-$ thymic Treg cell precursors into Foxp3$^+$ cells. In contrast to mice lacking c-Rel or Carma1, IκB$_{NS}$-deficient mice do not show reduced Treg precursor cells. Our results demonstrate that IκB$_{NS}$ critically regulates Treg cell development in the thymus and during gut inflammation, indicating that strategies targeting IκB$_{NS}$ could modulate the Treg cell compartment.

INTRODUCTION

Regulatory T (Treg) cells represent an essential T cell subset governing the maintenance of peripheral tolerance and immune homeostasis. Their capacity to suppress the activity of effector immune cells enables them to regulate the duration and intensity of the immune response and to prevent autoimmunity (Sakaguchi et al., 1995, 2007). Loss of functional Treg cells leads to a fatal autoimmune disease, termed immune dysregulation, polyendocrinopathy, enteropathy, X-linked syndrome (IPEX) in humans, or the homologous murine phenotype called *scurfy*. Both are caused by mutations in the transcription factor forkhead box P3 (Foxp3), which controls the development and phenotypic maintenance of Treg cells (Bennett et al., 2001; Brunkow et al., 2001; Hori et al., 2003).

The pool of Foxp3$^+$ Treg cells consists of induced (iTreg) and natural (nTreg) cells, the former being generated in peripheral lymphoid tissues by the conversion of naive CD4$^+$Foxp3$^-$ T cells into mature CD4$^+$Foxp3$^+$ cells. This process takes place in tissues such as the gut, which need high immune tolerance. This conversion requires T cell receptor (TCR) triggering as well as γ_c cytokine stimulation in order to enhance Foxp3 expression, Treg cell survival and expansion through the signal transducer and activator of transcription 5 (STAT5) (Burchill et al., 2007). Additionally, transforming growth factor-β (TGF-β) contributes to Treg cell maintenance and homeostasis via Smad3 signaling, as TGF-β1-deficient mice display reduced peripheral Treg cell numbers (Marie et al., 2005). In vitro, CD4$^+$ Foxp3$^-$ T cells are converted into Foxp3$^+$ cells by activation in the presence of TGF-β (Chen et al., 2003). However, in contrast to Treg cells developed in vivo, demethylation of CpG sites within the conserved noncoding sequence 2 (CNS2) of the *Foxp3* locus, also known as Treg-specific demethylation region (TSDR), does not occur (Floess et al., 2007; Zheng et al., 2010). As a result, the in vitro-induced Foxp3 expression is less stable (Polansky et al., 2008).

The essential signals for thymic nTreg cell development are TCR engagement, CD28 costimulation, and γ_c cytokine signals (Vang et al., 2008). Interestingly, comparison of TCR specificities between Foxp3$^-$ and Foxp3$^+$ T cells revealed that Treg cells express autoreactive TCRs (Apostolou et al., 2002; Hsieh et al., 2004; Jordan et al., 2001; Liston and Rudensky, 2007). These observations suggest that developing thymic nTreg cells escape negative selection. The currently most accepted "two-step model" of nTreg cell generation assumes that TCR-mediated signals in autoreactive CD4$^+$ cells induce expression of the interleukin-2 (IL-2) receptor α chain (CD25) and the glucocorticoid-induced-TNF-receptor (GITR), leading to the

development of nTreg precursor cells. Subsequently, Foxp3 is induced in CD4$^+$CD25$^+$GITR$^+$Foxp3$^-$ precursors by γ_c cytokines IL-2 and IL-15 (Burchill et al., 2008; Lio and Hsieh, 2008).

It was previously demonstrated that nTreg cell and iTreg cell development depend on the transcription factor NFκB (Barnes et al., 2009; Grigoriadis et al., 2011; Long et al., 2009; Ruan et al., 2009). Due to its impact on proliferation, cell death, and lymphocyte activation, NFκB is one of the most important eukaryotic transcription factor networks (Baldwin, 1996; Weil and Israël, 2006). Functional NFκB transcription factors are dimers formed by two members of the Rel-protein family. TCR stimulation involves p65, c-Rel and p50 (Bonizzi and Karin, 2004). The central event in NFκB signaling is the activation of the IκB kinase (IKK) complex (Hayden and Ghosh, 2012). This trimeric protein complex consists of two catalytic subunits, IKKα and IKKβ, and the scaffold protein IKKγ (Hayden and Ghosh, 2012). The IKKβ subunit of active IKK-complexes phosphorylates the cellular inhibitors of NFκB (termed IκBs), which sequester NFκB in the cytoplasm by masking their nuclear localization signals. Upon phosphorylation, classical IκBs are polyubiquitinated and degraded. Eventually, NFκB translocates into the nucleus and binds to κB-sites on the DNA (Perkins and Gilmore, 2006). Classical IκBs are distinguished from the atypical IκB proteins of the BCL-3 subfamily, such as BCL-3, IκBζ (encoded by the *Nfkbiz* gene), and IκB$_{NS}$ (encoded by the *Nfkbid* gene) (Hayden and Ghosh, 2012). The latter proteins are not degraded after NFκB activation but are highly induced and, notably, act as transcriptional modulators with inductive and repressive capacities by binding to NFκB transcription factors in the nucleus (Ghosh and Hayden, 2008; Mankan et al., 2009).

Essential for nTreg cell lineage commitment is a protein kinase C-Θ-activated complex formed by Carma1 (encoded by the *Card11* gene), BCL-10, and MALT1 (CBM) (Barnes et al., 2009; Thome, 2004). Notably, *Card11*-deficient mice lack thymic CD25$^+$GITR$^+$Foxp3$^-$ Treg precursor cells, leading to a massive reduction in mature Treg cell numbers (Molinero et al., 2009) Because the CBM complex is proximal to the TCR, constitutively active IKKβ rescues the induction of Foxp3 in *Card11*-deficient Treg precursor cells (Long et al., 2009). Regarding distal NFκB signaling, it was shown that c-Rel controls Treg cell precursor generation and drives Foxp3 expression by binding to the promoter, CNS2, and CNS3 within the *Foxp3* locus (Hori, 2010; Hsieh, 2009; Isomura et al., 2009; Ruan et al., 2009; Zheng et al., 2010). However, whether or not atypical IκB proteins contribute to Treg cell development has not been analyzed yet.

The function of the BCL-3 subfamily protein IκB$_{NS}$ is almost completely unknown. It was first identified in autoreactive T cells of a mouse model for peptide-induced negative selection (Fiorini et al., 2002). However, neither distribution of CD4- and CD8-positive cells in the thymus and secondary lymphoid organs nor Vβ usage are affected by *Nfkbid* deficiency, but CD8$^+$ T cells of *Nfkbid*-deficient mice show reduced IL-2 and IFN-γ production after TCR triggering (Touma et al., 2007). We found that *Nfkbid*-deficient mice show a ~50% reduction of mature Treg cells. Unlike *Card11*-deficient mice, which display virtually no GITR$^+$CD25$^+$Foxp3$^-$ Treg precursor cells, *Nfkbid* deficiency leads to an increase of these precursor cells due to impaired transition into Foxp3$^+$ Treg cells. Moreover, IκB$_{NS}$ is transiently expressed during thymic nTreg cell development and drives Foxp3 induction by binding to the promoter and CNS3 via p50 and c-Rel. Taken together, our data identify IκB$_{NS}$ as a crucial regulator of Foxp3 induction during Treg cell development and Treg cell generation under chronic inflammatory conditions.

RESULTS

IκB$_{NS}$ Intrinsically Controls Treg Cell Numbers

A minority of autoreactive T cells is protected from negative selection, commences Foxp3 expression, and develops into nTreg cells (Lio and Hsieh, 2008; Liston and Rudensky, 2007). Consequently, the majority of Foxp3$^+$ Treg cells express TCRs recognizing self-peptides (Apostolou et al., 2002; Hsieh et al., 2004; Jordan et al., 2001; Liston and Rudensky, 2007). Although IκB$_{NS}$ was first identified in autoreactive T cells (Fiorini et al., 2002), negative selection is not altered in *Nfkbid*-deficient mice as demonstrated by the normal percentages and development of conventional T cells (see Figure S1A and S1B available online) (Kuwata et al., 2006; Touma et al., 2007). To uncover whether IκB$_{NS}$ is crucial for directing autoreactive T cells to the Treg cell lineage, we determined Treg cell frequencies by intracellular staining of Foxp3 in *Nfkbid*-deficient and wild-type (WT) mice. *Nfkbid*-deficient mice displayed a reduction of Treg cells in thymus, spleen, mesenteric, and peripheral lymph nodes (Figure 1A and 1B). In line with reduced Treg cell frequencies, their total number was diminished in *Nfkbid*-deficient mice as well (Figure 1B). Numbers and frequencies of the total CD4$^+$ T cell compartment were comparable between *Nfkbid*-deficient and WT mice (Figure 1C). Moreover, frequencies of Foxp3$^+$ Treg cells in WT, heterozygous, and *Nfkbid*-deficient littermate mice were significantly different in thymus, mesenteric, and peripheral lymph nodes, indicating that IκB$_{NS}$ modulates the generation of Treg cells in a dose-dependent manner (Figure S1C) without affecting the total CD4$^+$ T cell compartment (Figure S1D). In addition, the activation status of conventional T cells assessed by CD62L and CD44 expression was similar in *Nfkbid*-deficient mice (Figure S1E and S1F).

To determine whether IκB$_{NS}$ affects Treg cell generation by extrinsic factors or via an intrinsic mechanism, we generated mixed bone marrow chimeric mice. The composition of the CD4$^+$Foxp3$^+$ Treg cell compartment by *Nfkbid*$^{+/+}$Thy1.1 and *Nfkbid*$^{-/-}$Thy1.2 cells was analyzed by flow cytometry 8 weeks after bone marrow transfer (Figure 1D). *Nfkbid*$^{-/-}$Thy1.2 Treg cells were virtually not detectable, whereas the CD4$^+$*Nfkbid*$^{+/+}$ Thy1.1 compartment exhibited normal Treg cell frequencies of about 9% (Figure 1E). Because the presence of WT T cells could not overcome *Nfkbid* deficiency in mixed bone marrow chimeric mice, IκB$_{NS}$ intrinsically regulates Treg cell development.

IκB$_{NS}$ Deficiency Neither Enhances Treg Cell Apoptosis nor Reduces Treg Cell Proliferation

NFκB is known to support proliferation and survival (Hayden and Ghosh, 2012). To determine whether the reduced amount of Treg cells in *Nfkbid*-deficient mice is caused by impaired proliferation or enhanced apoptosis, *Nfkbid*-deficient mice were crossed with Foxp3$^{DTR\text{-}eGFP}$ reporter mice, allowing analysis of nonfixed Treg cells. Similar to nonreporter mice, Treg cell frequencies were reduced in *Nfkbid*$^{-/-}$Foxp3$^{DTR\text{-}eGFP}$ compared

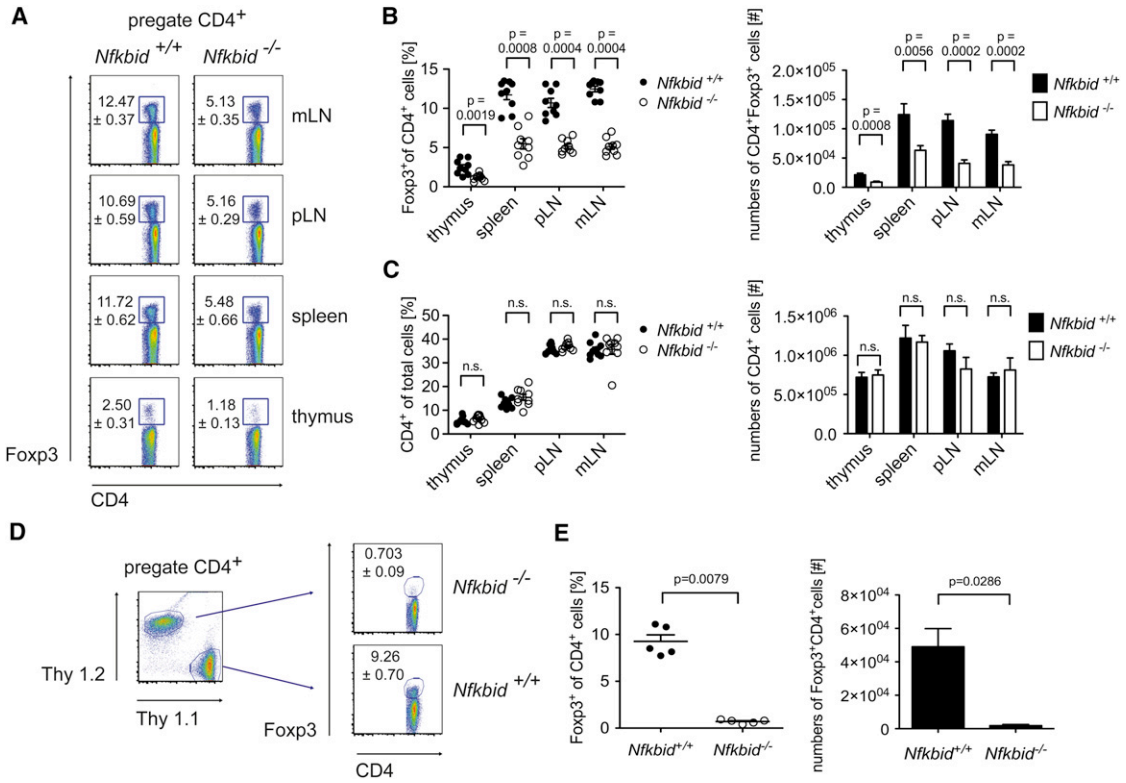

Figure 1. $I\kappa B_{NS}^{-/-}$ Mice Display Reduced Treg Cell Frequencies and Numbers

(A) Flow cytometric analysis of Treg cell frequencies in the spleen, thymus, and mesenteric (mLN) and peripheral lymph nodes (pLN) of WT (*Nfkbid*$^{+/+}$) and $I\kappa B_{NS}$-deficient (*Nfkbid*$^{-/-}$) mice assessed by intracellular Foxp3 staining. Representative pseudocolor dot plots of Foxp3$^+$ Treg cells within CD4$^+$ cells in 8-week-old mice are shown. Numbers indicate the percentages of gated CD4$^+$Foxp3$^+$ Treg cells.

(B) Percentages and absolute numbers of Foxp3$^+$ Treg cells within CD4$^+$ cells in spleen, thymus, and peripheral and mesenteric lymph nodes of WT (*Nfkbid*$^{+/+}$) and $I\kappa B_{NS}$-deficient (*Nfkbid*$^{-/-}$) mice (n = 9 each) are shown.

(C) Flow cytometric analysis of the CD4$^+$ T cell compartment. Percentages and absolute numbers of CD4 cells in spleen, thymus, and peripheral and mesenteric lymph nodes of *Nfkbid*$^{+/+}$ and *Nfkbid*$^{-/-}$ mice (n = 9 each) are shown.

(D) Mixed bone marrow chimeric mice were analyzed 8 weeks after transfer of *Nfkbid*$^{+/+}$Thy1.1 and *Nfkbid*$^{-/-}$Thy1.2 bone marrow cells into sublethally irradiated WT recipient mice. Representative pseudocolor dot plots of splenic CD4$^+$Thy1.1 and CD4$^+$Thy1.2 cells and of CD4$^+$Foxp3$^+$ cells pregated to *Nfkbid*$^{+/+}$Thy1.1$^+$ or *Nfkbid*$^{-/-}$Thy1.2$^+$ cells are shown.

(E) Percentages (left panel) and absolute numbers (right panel) of splenic CD4$^+$Foxp3$^+$ Treg cells of *Nfkbid*$^{+/+}$ and *Nfkbid*$^{-/-}$ origin in bone marrow chimeras. For (B), (C), and (E), each symbol indicates an individual mouse. Horizontal lines represent the mean; error bars represent SEM. Statistical analyses were performed by two-tailed Mann-Whitney tests; $\alpha < 0.05$; n.s., not significant.

to *Nfkbid*$^{+/+}$Foxp3$^{DTR\text{-}eGFP}$ mice (Figure S2A). The rates of apoptosis, analyzed by the frequencies of early apoptotic (AnnexinV$^+$7AAD$^-$) and late apoptotic (AnnexinV$^+$7AAD$^+$) CD4$^+$GFP$^+$ Treg cells were comparable between WT and *Nfkbid*$^{-/-}$ mice (Figures 2A and 2B; Figure S2B). To corroborate this data, we also measured Treg cell viability by staining with tetramethylrhodamine ethyl ester (TMRE). Cells that have lost mitochondrial membrane integrity during early apoptosis are TMRE low. In agreement with AnnexinV/7AAD analyses, no significant difference between Treg cells of *Nfkbid*$^{+/+}$Foxp3^{DTReGFP} and *Nfkbid*$^{-/-}$Foxp3^{DTReGFP} mice was detectable (Figure 2C). Also, cell death of CD4$^+$Foxp3$^-$ conventional T cells was unaffected by *Nfkbid* deficiency (Figures 2A–2C).

Previous studies reported reduced proliferation of *Nfkbid*-deficient conventional T cells upon stimulation via CD3 and CD28 in vitro (Touma et al., 2007). Thus, the possibility of defective Treg cell proliferation was investigated by analyzing the expression of the Ki67 proliferation marker, which is downregulated in the G0-arrest of the cell cycle. Remarkably, Foxp3$^+$ Treg cells of the thymus and peripheral lymphoid organs from *Nfkbid*-deficient mice displayed increased amounts of Ki67-positive cells (Figures 2D and 2E). To confirm this data, we fed mice orally with BrdU, which is incorporated into the DNA during the S phase. Corresponding to the Ki67 data, peripheral *Nfkbid*-deficient Treg cells displayed increased BrdU incorporation (Figures S2C and S2D). Proliferation of conventional T cells was unaffected in vivo (Figures 2D and 2E; Figures S2C and S2D). Compendious, *Nfkbid*-deficient mice displayed neither increased basal apoptosis nor decreased proliferation of Treg cells but a certain increase in proliferation.

$I\kappa B_{NS}$-Deficient Naive T Cells Display Reduced Foxp3 Induction upon TGF-β Treatment or Adoptive Transfer into Rag1$^{-/-}$ Mice

As steady state generation of Treg cells was impaired upon *Nfkbid* deficiency, we analyzed whether $I\kappa B_{NS}$ affects iTreg cell

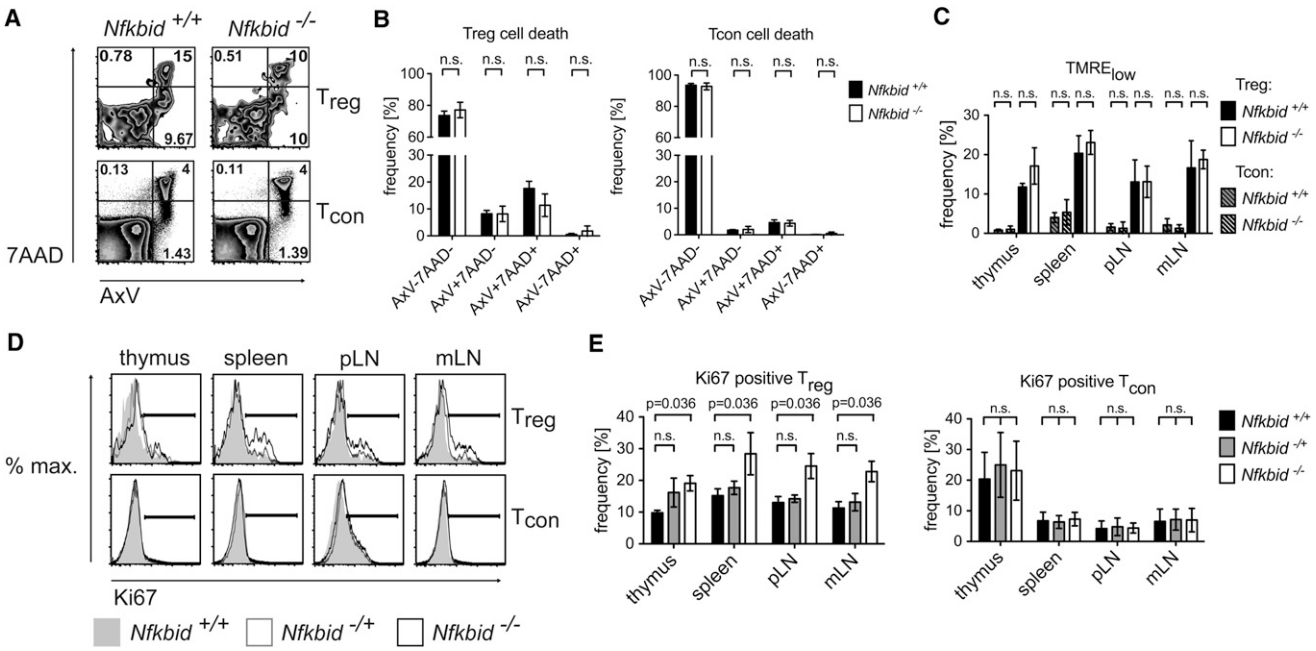

Figure 2. IκB$_{NS}$-Deficient Treg Cells Undergo Enhanced Proliferation but Display Normal Apoptosis

(A) Representative zebra plots of the AnnexinV/7AAD distribution of thymic GFP$^+$ Treg and GFP$^-$ Tcon cells from *Nfkbid*$^{+/+}$Foxp3$^{DTR\text{-}eGFP}$ and *Nfkbid*$^{-/-}$Foxp3$^{DTR\text{-}eGFP}$ mice.

(B) Statistical summary of apoptosis among GFP$^+$ Treg cells and GFP$^-$ Tcon cells from the thymus of *Nfkbid*$^{+/+}$Foxp3$^{DTR\text{-}eGFP}$ (filled bars) and *Nfkbid*$^{-/-}$Foxp3$^{DTR\text{-}eGFP}$ (open bars) mice is shown (n = 6 for each). AxV$^-$/7AAD$^-$ cells are living cells, AxV$^+$/7AAD$^-$ are early apoptotic cells, and AxV$^+$/7AAD$^+$ are late apoptotic cells.

(C) CD4$^+$Foxp3$^+$ Treg cells and CD4$^+$Foxp3$^-$ Tcon cells from spleen, thymus, and peripheral and mesenteric lymph nodes from *Nfkbid*$^{+/+}$Foxp3$^{DTR\text{-}eGFP}$ and *Nfkbid*$^{-/-}$Foxp3$^{DTR\text{-}eGFP}$ mice (n = 6 for each) were stained with TMRE to assess mitochondrial membrane potential. Statistical summary of the percentages of TMRE low (early apoptotic) cells is shown.

(D) Flow cytometric analysis of Ki67 expression in pregated CD4$^+$Foxp3$^+$ Treg cells and CD4$^+$Foxp3$^-$ Tcon cells from thymi, spleens, and peripheral and mesenteric lymph nodes. Representative Ki67-histogram overlays of cells from WT, heterozygous, and *Nfkbid*-deficient mice are shown.

(E) Statistical analysis of Ki67-positive cells among pregated CD4$^+$Foxp3$^+$ Treg cells and CD4$^+$Foxp3$^-$ Tcon cells of WT (*Nfkbid*$^{+/+}$; n = 3), heterozygous (*Nfkbid*$^{-/+}$; n = 4), and IκB$_{NS}$-deficient (*Nfkbid*$^{-/-}$; n = 5) mice are shown. For (B), (C), and (E) error bars display SEM. Statistical analyses were performed by two-tailed Mann-Whitney tests; $\alpha < 0.05$. n.s., not significant.

generation. Purified *Nfkbid*-deficient CD4$^+$CD62L$^+$CD25$^-$ naive T cells stimulated in vitro with low dose TGF-β in the presence of IL-2 commenced less Foxp3 expression compared to WT cells (Figure 3A). In the latter, IκB$_{NS}$ was induced during the early stages of TGF-β treatment (Figure S3A). High TGF-β concentrations, however, could overcome *Nfkbid* deficiency (Figure 3A). Staining of Ki67 revealed that the reduced amount of Foxp3 expressing cells was not the result of a proliferation defect (Figure 3B). Because in vitro differentiation implied impaired iTreg cell development, naive CD25$^-$CD4$^+$ T cells from WT or *Nfkbid*-deficient mice were adoptively transferred into *Rag1*$^{-/-}$ mice and Treg cell development in the gut was monitored. Flow cytometric analysis of lamina propria mononuclear cells (LPMC) revealed that CD4$^+$Foxp3$^+$ Treg cells barely developed from *Nfkbid*-deficient T cells, whereas approximately 5% of Treg cells originated from WT cells (Figure 3C). Accordingly, reduced frequencies and absolute numbers of Foxp$^+$ Treg cells were found in histological analyses (Figure 3D). In contrast, frequencies of total CD4$^+$ T cells in the LPMCs (Figure S3B) and IFN-γ producing cells were comparable between both groups (Figure 3E). However, *Rag1*$^{-/-}$ mice that had received *Nfkbid*-deficient T cells showed signs of severe colitis compared to control recipients, as revealed by stronger leukocyte infiltration of the large intestine (Figure 3F). Histopathology revealed severe inflammation in recipients of *Nfkbid*-deficient T cell, compared to recipients of WT T cells (Figure 3G). Accordingly, weight loss was exacerbated upon transfer of *Nfkbid*-deficient T cells (Figure 3H; Figure S3C), associated with increased colon shortening (Figure S3D) and severe diarrhea (Figure S3E). There was no statistical difference in the IL-6 release between both groups, but IFN-γ amounts in colon sections of *Nfkbid*-deficient T cell recipients were elevated, reflecting enhanced inflammation (Figure 3I). These experiments illustrate that IκB$_{NS}$ was required for Foxp3 induction upon TGF-β treatment and in adoptively transferred naive T cells.

IκB$_{NS}$ Does Not Modulate the Suppressor Function of Mature Treg Cells

So far, our data indicated impaired induction of Foxp3 in *Nfkbid*-deficient mice. To elucidate whether IκB$_{NS}$ is crucial for the function and maintenance of mature Treg cells, we examined the expression of Treg cell signature proteins CD25 (IL-2Rα), GITR, Foxp3, CD122 (IL-2Rβ), and CTLA-4 in Treg cells from

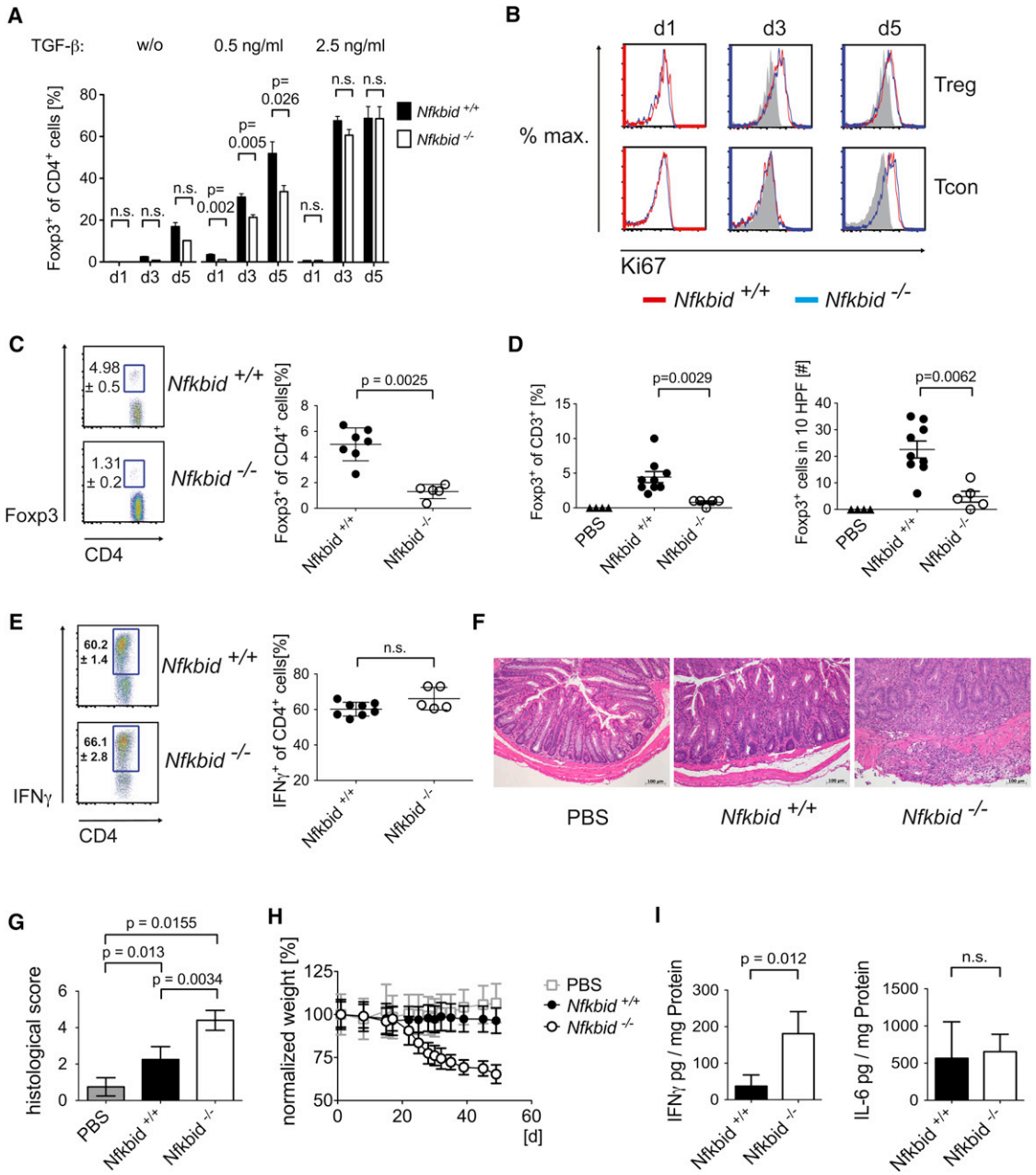

Figure 3. IκB$_{NS}$ Deficiency Impairs TGF-β-Mediated Induction of Foxp3 and iTreg Cell Development from Adoptively Transferred Tcon Cells

(A) Purified naive CD4$^+$CD62L$^+$CD25$^-$ T cells were treated with the indicated TGF-β concentrations in the presence of 10 ng/ml of IL-2. Statistical summary of Foxp3$^+$ cells analyzed by flow cytometry at days 1, 3, and 5 is shown. Filled bars represent WT; open bars indicate *Nfkbid*-deficient cells.

(B) Flow cytometry analyses of Ki67 expressing cells pregated to in vitro induced Foxp3$^+$ Treg cells and Foxp3$^-$ Tcon cells (n = 6). Red indicates WT; blue indicates *Nfkbid*-deficient cells. Grey represents Ki67 histogram at day 1.

(C) Treg cell induction in *Rag1*-deficient mice. The development of Treg cells from transferred *Nfkbid*$^{+/+}$ or *Nfkbid*$^{-/-}$ T cells, was analyzed by flow cytometry. Representative pseudocolor dot-plots of CD4$^+$Foxp3$^+$ Treg cells from the lamina propria pregated on CD4$^+$ T cells and statistical summary are shown.

(D) Frequencies and numbers of Treg cells of *Nfkbid*$^{+/+}$ (n = 9) or *Nfkbid*$^{-/-}$ (n = 5) origin in colon sections analyzed by immunohistology. Numbers of cells per 10 high power fields (HPF) are shown.

(E) Representative pseudocolor dot-plots of CD4$^+$IFN-γ$^+$ T cells pregated on CD4$^+$ T cells in the lamina propria from transferred *Nfkbid*$^{+/+}$ and *Nfkbid*$^{-/-}$ T cells and statistical summary are shown. Numbers indicate the percentages of gated CD4$^+$IFN-γ$^+$ T cells.

(F) Representative hematoxylin and eosin stained colon sections from *Rag1*-deficient mice injected with PBS, WT (*Nfkbid*$^{+/+}$) T cells, or IκB$_{NS}$-deficient (*Nfkbid*$^{-/-}$) T cells are shown. Scale bar represents 100 μm.

(G) Histopathology scoring from *Rag1*-deficient mice injected with PBS (n = 4), *Nfkbid*$^{+/+}$ (n = 8), or *Nfkbid*$^{-/-}$ (n = 5) T cells is shown. Diagram height indicates the mean; error bars represent SEM.

(H) Normalized weights of *Rag1*-deficient mice, injected with PBS (n = 4), *Nfkbid*$^{+/+}$ (n = 8), or *Nfkbid*$^{-/-}$ (n = 5) T cells are shown. Each point indicates the mean; error bars represent SEM.

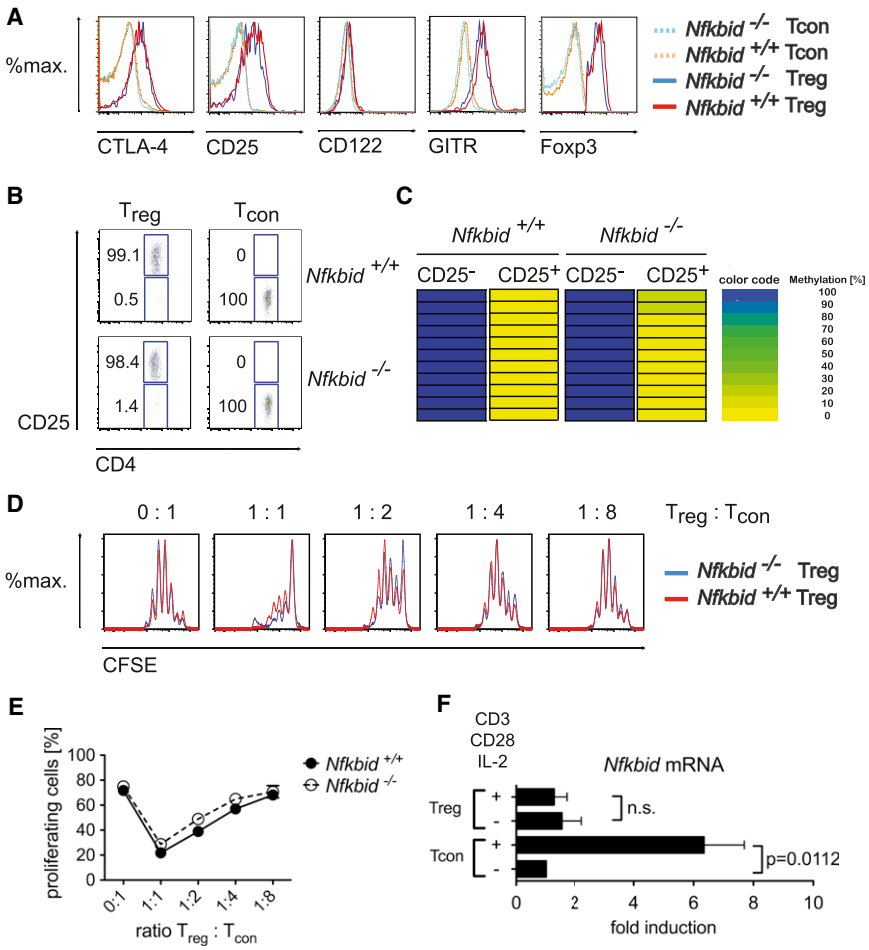

Figure 4. IκB$_{NS}$ Is Dispensable for the Phenotypic Maintenance of Regulatory T Cells

(A) Flow cytometric analysis of the expression of CD25, CD122, GITR, intracellular CTLA-4, and Foxp3. Representative histogram overlays of the indicated proteins of CD4$^+$Foxp3$^-$ Tcon cells and CD4$^+$Foxp3$^+$ Treg cells from the spleens of WT (*Nfkbid*$^{+/+}$) and IκB$_{NS}$-deficient (*Nfkbid*$^{-/-}$) mice are shown. Results are representative for three independent experiments.

(B) CD4$^+$CD25$^+$ Treg cells and CD4$^+$CD25$^-$ conventional T cells (Tcon) were sorted by flow cytometry to determine the CNS2/TSDR methylation status. Representative pseudocolor dot-plots of sorted cells from *Nfkbid*$^{+/+}$ and *Nfkbid*$^{-/-}$ male mice are shown. For each plot, the upper numbers indicate percentages of CD4$^+$CD25$^+$ Treg cells, and lower numbers indicate the percentages of CD4$^+$CD25$^-$ Tcon cells. Data are representative of WT (n = 4) and *Nfkbid*-deficient (n = 8) cells.

(C) Representative CNS2/TSDR methylation patterns of purified CD4$^+$CD25$^+$ Treg cells and CD4$^+$CD25$^-$ conventional T cells isolated as in (B). Amplicons are vertically arranged, each representing a single CpG-motif. Color code indicates the percentage of CNS2/TSDR methylation in the purified populations.

(D) The suppressive capacity of IκB$_{NS}$-deficient (*Nfkbid*$^{-/-}$) Treg cells compared to WT (*Nfkbid*$^{+/+}$) Treg cells was analyzed in vitro. Representative histogram overlays of CFSE-labeled WT conventional T cells (Tcon) cocultured for 3 days with Treg cells of *Nfkbid*$^{+/+}$ and *Nfkbid*$^{-/-}$ mice at the indicated ratios are shown.

(E) Percentage of proliferating Tcon cells during in vitro suppression assay as in (D) is shown. Data are representative for three independent triplicate measurements. Each symbol represents the mean; error bars represent the SD.

(F) Expression of IκB$_{NS}$ in purified CD4$^+$CD25$^+$ Treg cells and CD4$^+$CD25$^-$ Tcon cells, stimulated with 10 μg/ml anti-CD3, 5 μg/ml anti-CD28, and 10 ng/ml murine IL-2, analyzed by qPCR (n = 4). Error bars display SEM. Statistical analyses were performed by two-tailed Mann-Whitney tests; $\alpha < 0.05$; n.s., not significant.

Nfkbid-deficient and WT mice. Mean-fluorescent intensities were comparable in CD4$^+$Foxp3$^+$ cells obtained from thymus, spleen, peripheral, and mesenteric lymph nodes of *Nfkbid*-deficient and WT mice (Figure 4A; Figure S4A).

To further characterize mature Treg cells, we analyzed the epigenetic regulation of *Foxp3* by determining the methylation status of CNS2 in the *Foxp3* locus. CpG motifs in the CNS2 are fully methylated in conventional T cells and demethylated in Treg cells, a requirement for stable Foxp3 expression (Floess et al., 2007; Polansky et al., 2008). CD4$^+$CD25$^-$ conventional T cells and CD4$^+$CD25$^+$ Treg cells were purified from *Nfkbid*-deficient and WT mice (Figure 4B), purity of the isolated populations was determined by Foxp3 staining (Figure S4B), and the CNS2 methylation status was analyzed as previously reported (Floess et al., 2007; Polansky et al., 2008). Both genotypes displayed full CNS2 methylation in CD4$^+$CD25$^-$ T cells and similar demethylation of CNS2 in CD4$^+$CD25$^+$ Treg cells (Figure 4C; Figure S4C). Furthermore, the suppressive capacity of mature CD25$^+$ Treg cells in vitro isolated from *Nfkbid*-deficient and WT mice was comparable (Figures 4D and 4E). Taken together, we found no evidence that IκB$_{NS}$ affects phenotype or function of mature Treg cells.

IκB$_{NS}$ Is Expressed by Treg Precursor Cells and Controls Their Transition into Mature Treg Cells

A previous study reported that IκB$_{NS}$ is directly repressed by Foxp3 (Marson et al., 2007). Also, IκB$_{NS}$ expression was not inducible via CD3/CD28/IL-2 stimulation in purified Treg cells in contrast to conventional T cells (Figure 4F) (Touma et al., 2007). Because IκB$_{NS}$ is suppressed in mature Treg cells, but

(I) Release of proinflammatory cytokines was determined via bead-based assays. IFN-γ and IL-6 release in colon cultures of *Rag1*-deficient mice injected with *Nfkbid*$^{+/+}$ (n = 7) or *Nfkbid*$^{-/-}$ (n = 5) T cells are shown. Diagram height indicates the mean; error bars represent SEM. Numbers indicate the percentages of CD4$^+$Foxp3$^+$ Treg cells. For (A), (G), and (I), horizontal lines indicate the mean. For (C), (D), and (E), each symbol indicates an individual mouse. Horizontal lines represent the mean; error bars represent SEM. Statistical analyses were performed by two-tailed Mann-Whitney tests; $\alpha < 0.05$. n.s., not significant.

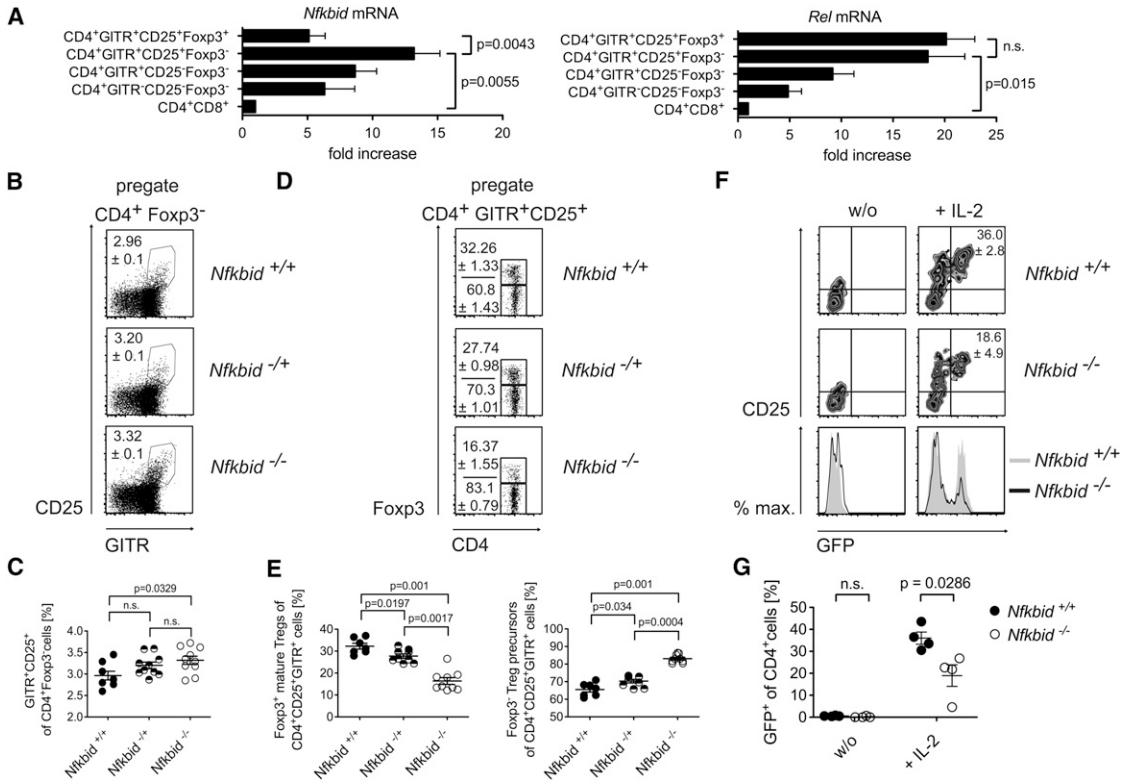

Figure 5. IκB$_{NS}$ Controls Transition of Immature Treg Precursor Cells into Mature Regulatory T Cells

(A) Expression of IκB$_{NS}$ (left panel) and c-Rel (right panel) in stages of nTreg cell development, analyzed by qPCR (n = 4).

(B) Representative dot-plots of CD25$^+$GITR$^+$ T cells pregated on the CD4$^+$CD8$^-$Foxp3$^-$ compartment in WT (*Nfkbid*$^{+/+}$), heterozygous (*Nfkbid*$^{-/+}$), and IκB$_{NS}$-deficient (*Nfkbid*$^{-/-}$) mice are shown. Numbers indicate the frequencies of gated Treg precursor cells.

(C) Statistical summary of the percentages of CD25$^+$GITR$^+$CD4$^+$CD8$^-$Foxp3$^-$ Treg precursor cells in the thymi of *Nfkbid*$^{+/+}$ (n = 8), *Nfkbid*$^{-/+}$ (n = 10), and *Nfkbid*$^{-/-}$ (n = 10) mice is shown.

(D) Percentages of Foxp3$^-$ Treg precursor cells and Foxp3$^+$ mature Treg cells within the thymic CD8$^-$CD4$^+$CD25$^+$GITR$^+$ compartment were determined by flow cytometry. Representative dot-plots of cells from *Nfkbid*$^{+/+}$, *Nfkbid*$^{-/+}$, and *Nfkbid*$^{-/-}$ mice are shown. Lower numbers indicate percentages of CD4$^+$Foxp3$^-$ precursor cells, upper numbers indicate percentages of CD4$^+$Foxp3$^+$ Treg cells.

(E) Summary of percentages of Treg precursor cells (right panel) and mature Treg cells (left panel) within the thymic CD8$^-$CD4$^+$CD25$^+$GITR$^+$ subset in *Nfkbid*$^{+/+}$ (n = 7), *Nfkbid*$^{-/+}$ (n = 9), and *Nfkbid*$^{-/-}$ (n = 9) mice is shown.

(F) Purified Treg precursor cells from *Nfkbid*$^{-/-}$Foxp3$^{DTR\text{-}eGFP}$ or *Nfkbid*$^{+/+}$Foxp3$^{DTR\text{-}eGFP}$ mice were stimulated with 100 ng/ml murine IL-2 or left untreated for 48 hr. Conversion of Treg precursor cells into mature Treg cells was determined by measuring GFP$^+$ cells. Representative zebra-plots and histograms of IL-2-treated and untreated precursors from *Nfkbid*$^{-/-}$Foxp3$^{DTR\text{-}eGFP}$ compared to *Nfkbid*$^{+/+}$Foxp3$^{DTR\text{-}eGFP}$ mice are shown. Numbers indicate percentages generated GFP expressing Treg cells.

(G) Statistical summary of the conversion of *Nfkbid*$^{-/-}$Foxp3$^{DTR\text{-}eGFP}$ and *Nfkbid*$^{+/+}$Foxp3$^{DTR\text{-}eGFP}$ Treg precursor cells into mature Treg cells after IL-2 treatment as in (F). For (C), (E), and (G), each symbol indicates an individual mouse. Horizontal lines represent the mean. For (A), (C), (E), and (G), error bars indicate the SEM. Statistical analyses were performed by two-tailed Mann-Whitney tests; $\alpha < 0.05$; n.s., not significant.

mixed bone-marrow chimeric mice demonstrated that IκB$_{NS}$ intrinsically regulates Treg cell development (Figures 1D and 1E), we speculated that IκB$_{NS}$ is expressed during thymic Treg cell maturation. To this end, we purified thymocytes according to the developmental sequence of the two-step model (Figure S5A). Strikingly, IκB$_{NS}$ was strongly expressed in CD4$^+$CD25$^+$GITR$^+$Foxp3$^-$ nTreg precursor cells and declined upon Foxp3 induction (Figure 5A). In contrast, c-Rel expression was maintained after transition of nTreg precursor cells into Foxp3$^+$ Treg cells (Figure 5A). Of note, *Card11*-deficient and *Rel*-deficient mice display a reduction of precursors contributing to the overall Treg cell reduction in these mice (Grigoriadis et al., 2011; Molinero et al., 2009). However, we found a significant increase in the frequencies of nTreg precursor cells in thymi of *Nfkbid*-deficient mice (Figures 5B and 5C), indicating impaired transition of precursor cells into Foxp3$^+$ Treg cells.

To explain this phenomenon, the distribution of Treg precursor cells and mature Treg cells within the CD8$^-$CD4$^+$CD25$^+$GITR$^+$ population was analyzed. Foxp3$^-$ Treg precursor cells made up the majority of this compartment in the thymi of *Nfkbid*-deficient mice, in contrast to heterozygous and WT littermates (Figures 5D and 5E). According to the two-step model, Foxp3 induction in precursor cells is induced by IL-2 (Lio and Hsieh, 2008). To determine whether IκB$_{NS}$ deficiency indeed regulates transition of precursors into mature Treg cells, *Nfkbid*$^{-/-}$Foxp3$^{DTR\text{-}eGFP}$ and *Nfkbid*$^{+/+}$Foxp3$^{DTR\text{-}eGFP}$ reporter mice were used for IL-2-induced transition in vitro. Of note,

increased frequencies of GFP$^-$ Treg precursor cells were detected in *Nfkbid*$^{-/-}$Foxp3$^{DTR\text{-}eGFP}$ mice as in nonreporter mice excluding influences by the BAC transgene (Figure S5B). Upon IL-2 treatment of isolated CD8$^-$CD4$^+$GITR$^+$CD25$^+$GFP$^-$, Treg precursor cells less than 25% of *Nfkbid*-deficient in contrast to about 40% of *Nfkbid*$^{+/+}$ precursor cells cells developed into mature Foxp3$^+$ Treg cells (Figures 5F and 5G). Despite a mild difference in CD122 expression, steady-state phosphorylation of STAT5 in Treg precursor cells from WT and *Nfkbid*-deficient mice was similar, (Figure S5C), indicating normal IL-2 signal transduction in *Nfkbid*-deficient T cells.

IκB$_{NS}$ Interacts with p50 and c-Rel and Binds to the Foxp3 Promoter and CNS3

To investigate how IκB$_{NS}$ controls Treg cell development, we asked whether it binds directly to the *Foxp3* locus. Because numbers of Treg precursor cells were too low to allow for biochemical analyses, *Nfkbid* induction was analyzed in thymic CD4$^+$GITR$^-$CD25$^-$Foxp3$^-$ cells, which give rise to Treg precursor cells, and peripheral CD4$^+$CD25$^-$ cells. *Nfkbid* was induced by TCR triggering in thymic and peripheral CD4$^+$ T cells, but not by CD28 or IL-2 costimulation alone (Figure 6A). Thus, the latter cell type was chosen to study the interaction of IκB$_{NS}$ with known NFκB components and the *Foxp3* locus. Fractionized cell lysis of PMA/ionomycin stimulated CD4$^+$CD25$^-$ T cells revealed nuclear translocation of p50, p65, and c-Rel (Figure 6B). IκB$_{NS}$ appeared within the first 4 hr of stimulation as a 35 kDa IκB$_{NS}$ protein in the cytoplasm and as two 70 kDa IκB$_{NS}$ isoforms in the nucleus, i.e., with similar kinetics as c-Rel (Figure 6B). Although the 70 kDa isoforms cannot be deduced from the *Nfkbid* gene structure and have not been reported before, their absence in *Nfkbid*-deficient cells indicates that these isoforms are *Nfkbid* gene products (data not shown). Because IκB$_{NS}$ does not contain a DNA-binding motif, the protein requires interaction with NFκB subunits to associate with DNA. Coimmunoprecipitations (coIP) using cytoplasmic and nuclear extracts of stimulated CD4$^+$CD25$^-$ T cells revealed that cytoplasmic 35 kDa IκB$_{NS}$ did not interact with any NFκB subunit (Figure 6C). Strong coprecipitation of IκB$_{NS}$ with p50 and to a weaker extent with c-Rel was found in nuclear extracts, but interaction with p65 was not observed (Figure 6C).

NFκB binding to the promoter, CNS2, and CNS3 of the *Foxp3* gene has been previously described (Figure S6A) (Long et al., 2009; Ruan et al., 2009; Zheng et al., 2010). We found by native chromatin immunoprecipitations (ChIP) binding of IκB$_{NS}$ to the *Foxp3* promoter and CNS3 (Figures 6D and 6E). Furthermore, pull-down analyses revealed binding of IκB$_{NS}$, c-Rel, and p50 to the single κB site of CNS3 (Figure 6F). Two DNA sequences of the IL-2 promoter, a classical κB-binding site and a CD28-responsive element known to bind p50 and c-Rel, respectively, served as controls (Touma et al., 2007). The consequence of IκB$_{NS}$ deficiency for the transcriptional activity was addressed in T cells isolated from WT and *Nfkbid*-deficient mice using a luciferase-based reporter gene assay, as previously reported (Polansky et al., 2010; Zheng et al., 2010). Of note, the *Foxp3* promoter alone has only minimal transcriptional activity (Zheng et al., 2010). Using a construct, in which the promoter is fused to CNS3, transcription is not enhanced (Figure 6G), because the pioneer element functions as a chromatin opener of the *Foxp3* locus (Zheng et al., 2010). However, when the promoter was fused to the CNS2 enhancer segment, strong luciferase activity was observed (Zheng et al., 2010), which was reduced by about 50% in *Nfkbid*-deficient T cells (Figure 6G), further emphasizing that IκB$_{NS}$ directly regulates Foxp3 induction.

DISCUSSION

Recent studies revealed the importance of NFκB signaling for Treg cell generation, but the participating proteins remain largely unknown (Lu and Rudensky, 2009). This study shows that the atypical IκB protein IκB$_{NS}$ regulates Foxp3 expression, leading to a reduction of mature Treg cells in *Nfkbid*-deficient mice by about 50%. Furthermore, we demonstrated IκB$_{NS}$ expression during thymic nTreg cell development and upon TGF-β treatment of naive cells. Consequently, *Nfkbid*-deficient T cells showed reduced induction of Foxp3 when stimulated with low doses of TGF-β. Moreover, fewer Foxp3 expressing cells developed from adoptively transferred *Nfkbid*-deficient conventional cells. Frequencies of IFN-γ-producing effector T cells and total CD4 cells were normal. Thus, it is conceivable that impaired Treg cell generation caused the observed exacerbated colitis in recipients of *Nfkbid*-deficient cells, although we cannot completely exclude that altered Th1 cell activity contributes to this phenotype. Because expression of Treg cell signature proteins, TSDR methylation, and suppressive activity of Treg cells from *Nfkbid*-deficient and WT mice were comparable, IκB$_{NS}$ seems dispensable for maintenance of mature Treg cells. This is supported by the fact that *Nfkbid* itself is suppressed in mature Treg cells (Marson et al., 2007). Interestingly, *Nfkbid*-deficient Treg cells display mildly stronger proliferation compared to WT cells as assessed by Ki67 and BrdU staining. Although apoptosis is not increased in *Nfkbid*-deficient Treg cells, their absolute number is reduced. Most likely, mature *Nfkbid*-deficient Treg cells try to compensate their reduced generation by undergoing enhanced homeostatic proliferation. However, because the starting population is massively reduced, this is insufficient to restore normal Treg cell numbers before they undergo apoptosis.

Previous work concluded that Carma1 is necessary for the generation of Treg precursor cells, which are almost completely abolished in *Card11*-deficient mice (Barnes et al., 2009; Molinero et al., 2009). Similarly, *Rel*-deficient mice display less Treg precursor cells (Grigoriadis et al., 2011). We present evidence that IκB$_{NS}$, which is strongly expressed in Treg precursor cells, triggers the transition of precursor cells into Foxp3$^+$ Treg cells but is dispensable for precursor development. As further development is delayed, IκB$_{NS}$ deficiency causes an increase in precursor cells. NFκB binds to the *Foxp3* locus in Foxp3$^-$ conventional cells upon TCR triggering, even without a Foxp3 inducing stimulus (Long et al., 2009; Ruan et al., 2009). Accordingly, current models suggest NFκB to be a pioneer transcription factor activated upon initial TCR stimulation. Thus, in addition to the direct control of Foxp3 expression, NFκB renders the locus responsive for secondary transcription factors activated, e.g., by γ$_c$ cytokines (Hori, 2010; Hsieh, 2009). An obvious consequence of this model is reduced responsiveness of Treg precursor cells to γ$_c$ cytokines, when the instructive NFκB signal is impaired. In line with this prediction, we demonstrated that IκB$_{NS}$ is required for Foxp3 induction upon IL-2 treatment of

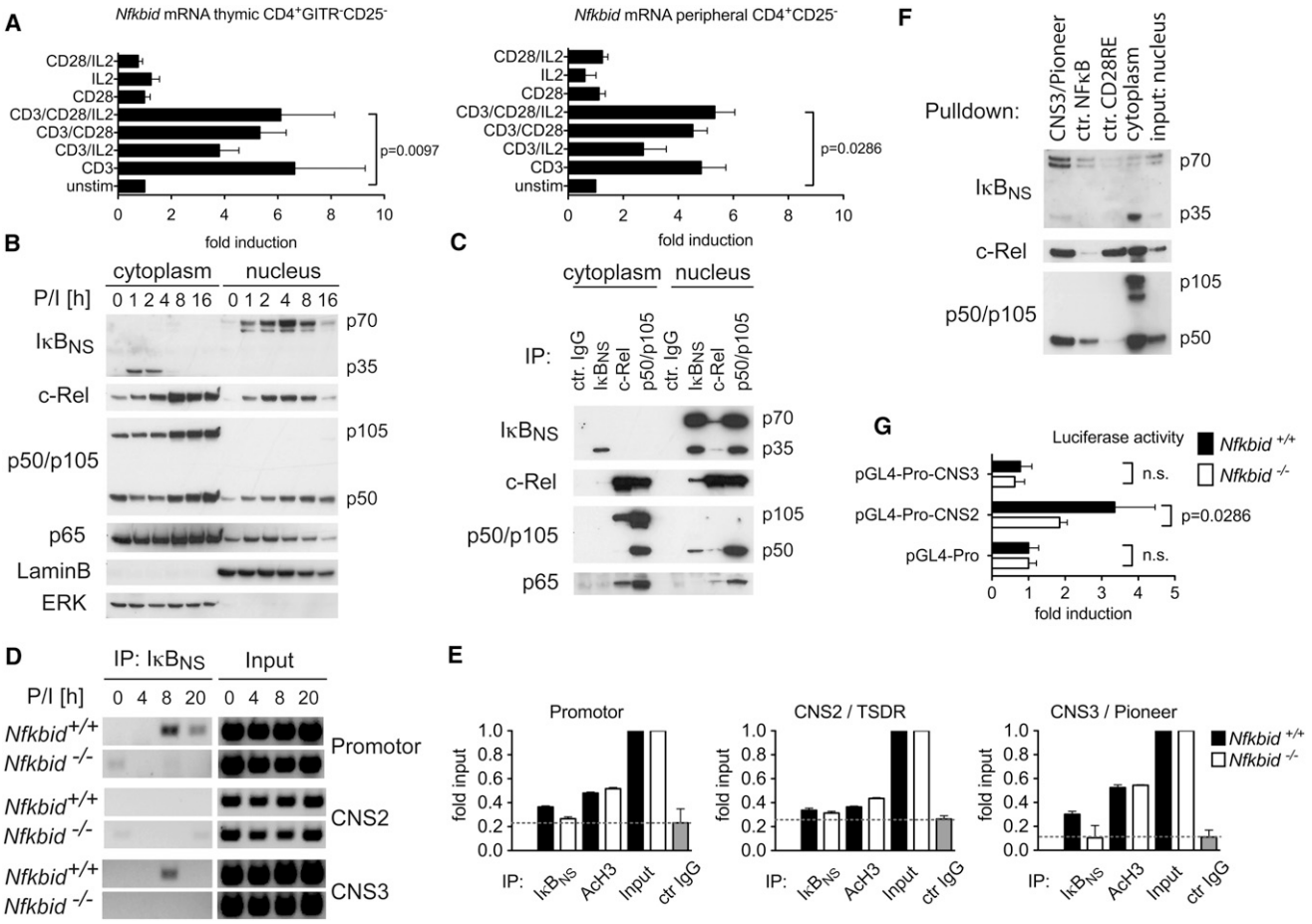

Figure 6. IκB$_{NS}$ Binds to the *Foxp3* Promoter and CNS3, Is Induced by CD3 Mediated Signals, and Interacts with c-Rel and p50

(A) Expression of IκB$_{NS}$ in thymic CD4$^+$CD25$^-$GITR$^-$Foxp3$^-$ cells (left panel, n = 6) and peripheral CD4$^+$CD25$^-$ cells (right panel, n = 4) stimulated with the indicated combinations of 10 μg/ml anti-CD3, 5 μg/ml anti-CD28, or 10 ng/ml IL-2, respectively, analyzed by qPCR.

(B) NFκB activation was analyzed by immunoblotting of cytoplasmic and nuclear extracts. CD4$^+$CD25$^-$ Tcon cells were purified by FACS, expanded for 7 days in vitro, and, subsequently, stimulated with 1 μM ionomycin and 10 ng/ml PMA for the indicated time periods.

(C) CD4$^+$CD25$^-$ Tcon cells were expanded as described above and stimulated for 4 hr with PMA/ionomycin. Cytoplasmic and nuclear extracts were used for immunoprecipitations (IP) of IκB$_{NS}$, c-Rel, and p50/p105 with rabbit polyclonal antibodies. CoIP of the proteins was analyzed via immunoblotting.

(D) ChIP using an IκB$_{NS}$-specific rabbit polyclonal antibody in WT and *Nfkbid*-deficient CD4$^+$CD25$^-$ Tcon cells, stimulated for the indicated times with PMA/ionomycin. Representative PCR results of amplification of promoter, CNS2, and CNS3 are shown. *Nfkbid*-deficient cells served as controls.

(E) Representative qPCR analysis of chromatin IPs, corresponding to (D). Anti-Acetyl-Histone 3 antibody and input served as positive controls, unspecific rabbit IgG as a negative control.

(F) Interaction of IκB$_{NS}$ with the single κB site of the CNS3/pioneer element was analyzed by DNA pull-down. Nuclear extracts were prepared from expanded and stimulated CD4$^+$CD25$^-$ T cells as described in (B) and (C). Eluted proteins were analyzed via immunoblot. Nuclear and cytoplasmic extracts were used as stimulation controls. Classical NFκB binding site and the CD28 response element of the IL-2 locus, known to bind IκB$_{NS}$/p50 and c-Rel, respectively, were used as interaction controls.

(G) Luciferase-based reported gene assay using constructs containing regulatory elements of the *Foxp3* locus fused to the *Foxp3* promoter. Fold induction of the indicated constructs, nucleofected into WT (filled bars; n = 3), and IκB$_{NS}$-deficient (empty bars; n = 3) CD4$^+$CD25$^-$ T cells are shown. For (B), (C), (D), and (F), each blot is representative of at least three independent experiments. For (A), (E), and (G), error bars represent SEM. Statistical analyses were performed by two-tailed Mann-Whitney tests; $\alpha < 0.05$.

Treg precursor cells. Similar findings were recently reported for c-Rel, demonstrating that it functions in precursor generation as well as Foxp3 induction (Grigoriadis et al., 2011). However, in *Rel*-deficient precursors phosphorylation of STAT5 was impaired (Grigoriadis et al., 2011), whereas we found no evidence for altered phosphorylation of STAT5 in *Nfkbid*-deficient precursors. Regarding the functional differences of Carma1, c-Rel and IκB$_{NS}$, it is conceivable that those proteins are sequentially activated during nTreg cell generation. The activity of Carma1 is essential for Treg cell precursor generation (Barnes et al., 2009), IκB$_{NS}$ forces transition into mature Treg cells, and c-Rel participates in both processes (Grigoriadis et al., 2011). Therefore, NFκB activity critically regulates both checkpoints of the two-step model.

Binding of c-Rel to the promoter, CNS2, and CNS3 of the *Foxp3* locus has been previously reported (Figure S6A) (Long

et al., 2009; Ruan et al., 2009; Zheng et al., 2010). We detected binding of IκB$_{NS}$ to the promoter and CNS3 using ChIP. Moreover, transcriptional activity in *Nfkbid*-deficient T cells is reduced as assessed by reporter gene assays. Thus, binding of IκB$_{NS}$ to the promoter is necessary for full transcriptional activation of the *Foxp3* locus. Via DNA pull-down experiments, we additionally found binding of IκB$_{NS}$, p50, and c-Rel to CNS3. Because this segment is thought to be an origin of chromatin opening during Foxp3 induction, it is likely that IκB$_{NS}$ participates in that process. This idea is further supported by previous studies, which demonstrated that atypical IκBs interact with chromatin remodeling enzymes (Dechend et al., 1999). Because Foxp3 is the master transcription factor for Treg cell development and function, we conclude that regulation of Foxp3 expression is a major mechanism of IκB$_{NS}$ driving Treg cell development though we cannot formally exclude that indirect mechanisms involving other IκB$_{NS}$ target genes may exist.

In summary, our data highlight the importance of the NFκB regulator IκB$_{NS}$ for the development of thymic derived and induced Treg cells. A recent study illustrated that Th17 cell development and function depends on the BCL-3 class protein IκBζ, which shows high sequence similarity to IκB$_{NS}$ (Okamoto et al., 2010). In line with our findings, the group of atypical IκBs might be of particular importance for the development of distinct T helper cell subsets and could represent suitable pharmacological targets for the treatment of chronic inflammatory diseases.

EXPERIMENTAL PROCEDURES

Mice

C57BL/6 *Nfkbid*$^{-/-}$ mice and Foxp3$^{DTR\text{-}eGFP}$ (DEREG) mice have been described previously and were kept under pathogen-free conditions in the animal facilities of the Heinrich-Heine University Düsseldorf and Helmholtz-Centre for Infection Research (HZI), Braunschweig (Fiorini et al., 2002; Lahl et al., 2007). Thy1.1 congenic mice were bred in the animal facility at the HZI, Braunschweig. All animal experiments and breeding were performed in accordance with the guidelines of national and local authorities.

Generation of Mixed Bone Marrow Chimeric Mice

Bone marrow cells were isolated from femurs and tibias of donor animals (*Nfkbid*$^{-/-}$Thy1.2^{+} and *Nfkbid*$^{+/+}$Thy1.1^{+}). C57BL/6 WT recipient mice were coinjected with 5 × 10^{6} cells of each type 6 hr after sublethal irradiation (9 Gy). Eight weeks later, mice were sacrificed and analyzed by flow cytometry.

Adoptive Transfer Colitis

Freshly isolated CD4^{+}CD25^{-} T cells (5 × 10^{5}) from C57BL/6 and *Nfkbid*-deficient mice were injected intraperitoneally into *Rag1*$^{-/-}$ mice in 200 μl of PBS. CD4^{+}CD25^{-} T cells were isolated from spleens and lymph nodes by MACS separation (CD4 T Cell Isolation Kit, CD25-PE Kit, Miltenyi) to a purity of >98% as evaluated by flow cytometry. WT and IκB$_{NS}$-deficient mice were obtained from the animal facility of the Heinrich-Heine-University, Düsseldorf. *Rag1*$^{-/-}$ mice were bred at the animal facility of the Charité Berlin. All mice were kept under specific pathogen-free conditions and used according to local animal care regulations. Further information can be found online in the Supplemental Experimental Procedures.

Expansion CD4^{+}CD25^{-} T Cells

For IP analyses, DNA pull-downs and luciferase assays CD4^{+}CD25^{-} T cells were expanded in vitro. Purified T cells (4 × 10^{6}) were resuspended in 4 ml fully supplemented RPMI and stimulated with 1 μg/ml plate-bound anti-CD3 (145-2C11, Biolegend) and 2 μg/ml soluble CD28 (eBioscience) in the presence of 10 ng/ml murine IL-2 (402-ML, R&D) in a 6-well plate. On day 3, cells were transferred in a total of 15 ml fresh RPMI without antibodies and transferred into a 10 cm dish. Cells were used on day 6 for further experiments.

Luciferase Assays

Luciferase constructs of the *Foxp3* locus were a kind gift of Dr. Ye Zheng (Salk Institute for Biological Studies, La Jolla, CA, USA). Luciferase assays were performed as described (Polansky et al., 2010).

DNA Pull-Down

For DNA pull-down, cytoplasmic extracts of CD4^{+}CD25^{-} cells, stimulated for 4 hr with 10 ng/ml PMA and 1 μM ionomycin, were prepared as described above. Nuclear extracts were prepared using HGMK buffer (0.1% NP-40, 10 mM HEPES, pH7.9, 5 mM $MgCl_2$, 100 mM KCl, 1 mM DTT, 10% glycerol with inhibitors), and incubated overnight with 8 μg DNA-oligo, bound to paramagnetic streptavidin beads (MyOne Streptavidin C1, Invitrogen). Unbound proteins were removed and eluates were analyzed by immunoblotting. Sequences for DNA-oligos of CNS3, of the classical κB-site and of the CD28-responsive element of the IL-2 promoter, were taken from Zheng et al. (2010) and Touma et al. (2007).

Chromatin Immunoprecipitation

For ChIP analyses, WT and *Nfkbid*-deficient CD4^{+}CD25^{-} T cells were stimulated with 10 ng/ml PMA and 1 μM ionomycin for the indicated times. ChIP was performed using ChIP-IT® Express Enzymatic kit (Active Motif). The customer's procedure was modified to achieve ChIP without crosslinking. As a result, procedural steps to remove PFA and revert crosslinking were not performed. After elution of the precipitated promoter DNA, CNS2 and CNS3 were amplified by PCR. Primer sequences can be found online in the Supplemental Experimental Procedures.

SUPPLEMENTAL INFORMATION

Supplemental Information includes six figures and Supplemental Experimental Procedures and can be found with this article online at http://dx.doi.org/10.1016/j.immuni.2012.08.023.

ACKNOWLEDGMENTS

We thank Sabrina Schumann, Dominique Gollasch, Stephanie Grosch, and Inka Freise for their excellent technical assistance, Ralf Höcker for help with apoptosis experiments, and Alisha Walker for critically reading the manuscript. We are grateful to David Dettbarn and colleagues for excellent mouse husbandry. *Rag1*$^{-/-}$ mice were a kind gift from Thomas Blankenstein and Charité Berlin. DNA methylation experiments were developed and performed by Udo Baron and Sven Olek at Epiontis GmbH. We thank the Forschungskommission of the Heinrich-Heine University Düsseldorf for initial funding. Further support was provided by the Deutsche Forschungsgemeinschaft (SI 749/5-3) and the SFB 738/C-6 and SFB 685/B-7.

Received: November 14, 2011
Accepted: August 21, 2012
Published: November 29, 2012

REFERENCES

Apostolou, I., Sarukhan, A., Klein, L., and von Boehmer, H. (2002). Origin of regulatory T cells with known specificity for antigen. Nat. Immunol. *3*, 756–763.

Baldwin, A.S., Jr. (1996). The NF-kappa B and I kappa B proteins: new discoveries and insights. Annu. Rev. Immunol. *14*, 649–683.

Barnes, M.J., Krebs, P., Harris, N., Eidenschenk, C., Gonzalez-Quintial, R., Arnold, C.N., Crozat, K., Sovath, S., Moresco, E.M., Theofilopoulos, A.N., et al. (2009). Commitment to the regulatory T cell lineage requires CARMA1 in the thymus but not in the periphery. PLoS Biol. *7*, e51.

Bennett, C.L., Christie, J., Ramsdell, F., Brunkow, M.E., Ferguson, P.J., Whitesell, L., Kelly, T.E., Saulsbury, F.T., Chance, P.F., and Ochs, H.D.

(2001). The immune dysregulation, polyendocrinopathy, enteropathy, X-linked syndrome (IPEX) is caused by mutations of FOXP3. Nat. Genet. *27*, 20–21.

Bonizzi, G., and Karin, M. (2004). The two NF-kappaB activation pathways and their role in innate and adaptive immunity. Trends Immunol. *25*, 280–288.

Brunkow, M.E., Jeffery, E.W., Hjerrild, K.A., Paeper, B., Clark, L.B., Yasayko, S.A., Wilkinson, J.E., Galas, D., Ziegler, S.F., and Ramsdell, F. (2001). Disruption of a new forkhead/winged-helix protein, scurfin, results in the fatal lymphoproliferative disorder of the scurfy mouse. Nat. Genet. *27*, 68–73.

Burchill, M.A., Yang, J., Vogtenhuber, C., Blazar, B.R., and Farrar, M.A. (2007). IL-2 receptor beta-dependent STAT5 activation is required for the development of Foxp3+ regulatory T cells. J. Immunol. *178*, 280–290.

Burchill, M.A., Yang, J., Vang, K.B., Moon, J.J., Chu, H.H., Lio, C.W., Vegoe, A.L., Hsieh, C.S., Jenkins, M.K., and Farrar, M.A. (2008). Linked T cell receptor and cytokine signaling govern the development of the regulatory T cell repertoire. Immunity *28*, 112–121.

Chen, W., Jin, W., Hardegen, N., Lei, K.J., Li, L., Marinos, N., McGrady, G., and Wahl, S.M. (2003). Conversion of peripheral CD4+CD25- naive T cells to CD4+CD25+ regulatory T cells by TGF-beta induction of transcription factor Foxp3. J. Exp. Med. *198*, 1875–1886.

Dechend, R., Hirano, F., Lehmann, K., Heissmeyer, V., Ansieau, S., Wulczyn, F.G., Scheidereit, C., and Leutz, A. (1999). The Bcl-3 oncoprotein acts as a bridging factor between NF-kappaB/Rel and nuclear co-regulators. Oncogene *18*, 3316–3323.

Fiorini, E., Schmitz, I., Marissen, W.E., Osborn, S.L., Touma, M., Sasada, T., Reche, P.A., Tibaldi, E.V., Hussey, R.E., Kruisbeek, A.M., et al. (2002). Peptide-induced negative selection of thymocytes activates transcription of an NF-kappa B inhibitor. Mol. Cell *9*, 637–648.

Floess, S., Freyer, J., Siewert, C., Baron, U., Olek, S., Polansky, J., Schlawe, K., Chang, H.D., Bopp, T., Schmitt, E., et al. (2007). Epigenetic control of the foxp3 locus in regulatory T cells. PLoS Biol. *5*, e38.

Ghosh, S., and Hayden, M.S. (2008). New regulators of NF-kappaB in inflammation. Nat. Rev. Immunol. *8*, 837–848.

Grigoriadis, G., Vasanthakumar, A., Banerjee, A., Grumont, R., Overall, S., Gleeson, P., Shannon, F., and Gerondakis, S. (2011). c-Rel controls multiple discrete steps in the thymic development of Foxp3+ CD4 regulatory T cells. PLoS ONE *6*, e26851.

Hayden, M.S., and Ghosh, S. (2012). NF-κB, the first quarter-century: remarkable progress and outstanding questions. Genes Dev. *26*, 203–234.

Hori, S. (2010). c-Rel: a pioneer in directing regulatory T-cell lineage commitment? Eur. J. Immunol. *40*, 664–667.

Hori, S., Nomura, T., and Sakaguchi, S. (2003). Control of regulatory T cell development by the transcription factor Foxp3. Science *299*, 1057–1061.

Hsieh, C.S. (2009). Kickstarting Foxp3 with c-Rel. Immunity *31*, 852–853.

Hsieh, C.S., Liang, Y., Tyznik, A.J., Self, S.G., Liggitt, D., and Rudensky, A.Y. (2004). Recognition of the peripheral self by naturally arising CD25+ CD4+ T cell receptors. Immunity *21*, 267–277.

Isomura, I., Palmer, S., Grumont, R.J., Bunting, K., Hoyne, G., Wilkinson, N., Banerjee, A., Proietto, A., Gugasyan, R., Wu, L., et al. (2009). c-Rel is required for the development of thymic Foxp3+ CD4 regulatory T cells. J. Exp. Med. *206*, 3001–3014.

Jordan, M.S., Boesteanu, A., Reed, A.J., Petrone, A.L., Holenbeck, A.E., Lerman, M.A., Naji, A., and Caton, A.J. (2001). Thymic selection of CD4+CD25+ regulatory T cells induced by an agonist self-peptide. Nat. Immunol. *2*, 301–306.

Kuwata, H., Matsumoto, M., Atarashi, K., Morishita, H., Hirotani, T., Koga, R., and Takeda, K. (2006). IkappaBNS inhibits induction of a subset of Toll-like receptor-dependent genes and limits inflammation. Immunity *24*, 41–51.

Lahl, K., Loddenkemper, C., Drouin, C., Freyer, J., Arnason, J., Eberl, G., Hamann, A., Wagner, H., Huehn, J., and Sparwasser, T. (2007). Selective depletion of Foxp3+ regulatory T cells induces a scurfy-like disease. J. Exp. Med. *204*, 57–63.

Lio, C.W., and Hsieh, C.S. (2008). A two-step process for thymic regulatory T cell development. Immunity *28*, 100–111.

Liston, A., and Rudensky, A.Y. (2007). Thymic development and peripheral homeostasis of regulatory T cells. Curr. Opin. Immunol. *19*, 176–185.

Long, M., Park, S.G., Strickland, I., Hayden, M.S., and Ghosh, S. (2009). Nuclear factor-kappaB modulates regulatory T cell development by directly regulating expression of Foxp3 transcription factor. Immunity *31*, 921–931.

Lu, L.F., and Rudensky, A. (2009). Molecular orchestration of differentiation and function of regulatory T cells. Genes Dev. *23*, 1270–1282.

Mankan, A.K., Lawless, M.W., Gray, S.G., Kelleher, D., and McManus, R. (2009). NF-kappaB regulation: the nuclear response. J. Cell. Mol. Med. *13*, 631–643.

Marie, J.C., Letterio, J.J., Gavin, M., and Rudensky, A.Y. (2005). TGF-beta1 maintains suppressor function and Foxp3 expression in CD4+CD25+ regulatory T cells. J. Exp. Med. *201*, 1061–1067.

Marson, A., Kretschmer, K., Frampton, G.M., Jacobsen, E.S., Polansky, J.K., MacIsaac, K.D., Levine, S.S., Fraenkel, E., von Boehmer, H., and Young, R.A. (2007). Foxp3 occupancy and regulation of key target genes during T-cell stimulation. Nature *445*, 931–935.

Molinero, L.L., Yang, J., Gajewski, T., Abraham, C., Farrar, M.A., and Alegre, M.L. (2009). CARMA1 controls an early checkpoint in the thymic development of FoxP3+ regulatory T cells. J. Immunol. *182*, 6736–6743.

Okamoto, K., Iwai, Y., Oh-Hora, M., Yamamoto, M., Morio, T., Aoki, K., Ohya, K., Jetten, A.M., Akira, S., Muta, T., and Takayanagi, H. (2010). IkappaBzeta regulates T(H)17 development by cooperating with ROR nuclear receptors. Nature *464*, 1381–1385.

Perkins, N.D., and Gilmore, T.D. (2006). Good cop, bad cop: the different faces of NF-kappaB. Cell Death Differ. *13*, 759–772.

Polansky, J.K., Kretschmer, K., Freyer, J., Floess, S., Garbe, A., Baron, U., Olek, S., Hamann, A., von Boehmer, H., and Huehn, J. (2008). DNA methylation controls Foxp3 gene expression. Eur. J. Immunol. *38*, 1654–1663.

Polansky, J.K., Schreiber, L., Thelemann, C., Ludwig, L., Krüger, M., Baumgrass, R., Cording, S., Floess, S., Hamann, A., and Huehn, J. (2010). Methylation matters: binding of Ets-1 to the demethylated Foxp3 gene contributes to the stabilization of Foxp3 expression in regulatory T cells. J. Mol. Med. *88*, 1029–1040.

Ruan, Q., Kameswaran, V., Tone, Y., Li, L., Liou, H.C., Greene, M.I., Tone, M., and Chen, Y.H. (2009). Development of Foxp3(+) regulatory t cells is driven by the c-Rel enhanceosome. Immunity *31*, 932–940.

Sakaguchi, S., Sakaguchi, N., Asano, M., Itoh, M., and Toda, M. (1995). Immunologic self-tolerance maintained by activated T cells expressing IL-2 receptor alpha-chains (CD25). Breakdown of a single mechanism of self-tolerance causes various autoimmune diseases. J. Immunol. *155*, 1151–1164.

Sakaguchi, S., Wing, K., and Miyara, M. (2007). Regulatory T cells - a brief history and perspective. Eur. J. Immunol. *37* (*Suppl 1*), S116–S123.

Thome, M. (2004). CARMA1, BCL-10 and MALT1 in lymphocyte development and activation. Nat. Rev. Immunol. *4*, 348–359.

Touma, M., Antonini, V., Kumar, M., Osborn, S.L., Bobenchik, A.M., Keskin, D.B., Connolly, J.E., Grusby, M.J., Reinherz, E.L., and Clayton, L.K. (2007). Functional role for I kappa BNS in T cell cytokine regulation as revealed by targeted gene disruption. J. Immunol. *179*, 1681–1692.

Vang, K.B., Yang, J., Mahmud, S.A., Burchill, M.A., Vegoe, A.L., and Farrar, M.A. (2008). IL-2, -7, and -15, but not thymic stromal lymphopoeitin, redundantly govern CD4+Foxp3+ regulatory T cell development. J. Immunol. *181*, 3285–3290.

Weil, R., and Israël, A. (2006). Deciphering the pathway from the TCR to NF-kappaB. Cell Death Differ. *13*, 826–833.

Zheng, Y., Josefowicz, S., Chaudhry, A., Peng, X.P., Forbush, K., and Rudensky, A.Y. (2010). Role of conserved non-coding DNA elements in the Foxp3 gene in regulatory T-cell fate. Nature *463*, 808–812.